Rainbows and fogbows

David K. Lynch and Ptolemy Schwartz

The optics of rainbows and fogbows is investigated theoretically for monodisperse drops using Mie theory. Included in the calculations are a realistic solar illumination spectrum and the finite size of the sun. Drop sizes range from 3 to 300 μm ($3800 > X > 38$). Results are presented on the location, width, contrast, polarization, and color of both primary and secondary rainbows. Particular attention is given to rainbows formed in small drops (fogbows).

Key words: Rainbow, fogbow, scattering, Mie theory, atmospheric optics.

I. Introduction

Rainbows formed in clouds and fogs are called fogbows (also called mistbows, cloudbows, Bouguer's halo, Ulloa's ring, and white rainbows (see Plates 9–11) and look different from rainbows that originate in raindrops. Fogbows show paler, less saturated colors than rainbows and sometimes none at all. They are wider than ordinary rainbows and the scattering angle at which fogbows reach maximum intensity is a few degrees larger than the rainbow's 138° brightness maximum. These properties have been well documented, at least qualitatively, in the literature.[1,2] Ulloa[3] was the first to call attention to the fogbow.

Since fog is composed of drops whose radii are less than ~50 μm whereas raindrop radii may reach up to a few millimeters or more, the unusual appearance of the fogbow is correctly attributed to its origin in small drops. To put our understanding of fogbows on a quantitative level, we undertook a series of Mie theory calculations with three goals in mind: (1) supply a quantitative basis for understanding the transition between rainbows and fogbows, (2) begin a step-by-step building block approach to predicting the properties of natural rainbows, and (3) draw attention to a few effects that are not normally (and sometimes never) considered in interpreting rainbows.

In this paper we investigate the properties of rainbows using calculations from Mie theory for a range of monodisperse drops using both a realistic spectrum of solar illumination and finite angular extent of the sun. There has been little quantitative analysis of the progression from rainbows to fogbows, although our work has been guided in part by earlier studies of scattering by monodisperse[4,5] and polydisperse drops.[6]

II. Calculations

We calculated the integrated angular scatttering function (phase function) of light scattered from water drops, i.e., $I(\theta)$:

$$I(\theta) = KS_{\odot}(\theta) * \int S_{11}(a, \lambda, \theta) I_{\odot}(\lambda) d\lambda, \quad (1)$$

where θ is the scattering angle and $I(\theta)$ is the brightness; K is a scaling factor involving the observer's distance from the raindrop, which we eliminate from further discussion; $S_{\odot}(\theta)$ is the 1-D solar profile that is convolved (*) with the integral; $S_{11}(a,\lambda,\theta)$ is the scattering matrix element that is the ratio of the scattered-to-incident radiation for unpolarized incident light; S_{11} is a function of drop radius a, wavelength λ, scattering angle θ, and complex index of refraction n; $I_{\odot}(\lambda)$ is the incident solar flux; and $I(\theta)$ is proportional to photometric irradiance, i.e., W cm^{-2} sr^{-1}, and contains no color information because it has been integrated over wavelength.

The scattering calculations were performed using the code supplied by Bohren and Huffman[7] modified for double precision arithmetic. The wavelength-dependent complex index of refraction of water was taken from Irvine and Pollack.[8] The drop radius range of $3 < a < 300$ μm was chosen for this work because drops larger than 300 μm are distorted by aerodynamic pressure[9] or oscillate[10] and thus are not relevant to this work. Drops smaller than ~3 μm show no discernible rainbow. Calculations were performed over the scattering angles $110° < \theta < 160°$. The Nyquist sampling interval $\Delta\theta_N$ is $1.22\lambda/2a$, with λ being the wavelength of visible light, ~0.5 μm. The scattering angle interval $\Delta\theta$ was chosen to oversample the scattering function by

David Lynch is with Thule Scientific, 22914 Portage Circle Drive, Topanga, California 90290, and P. Schwartz is with University of Texas, Astronomy Department, Austin, Texas 78712-1083.

Received 29 October 1990.
0003-6935/91/243415-06$05.00/0.

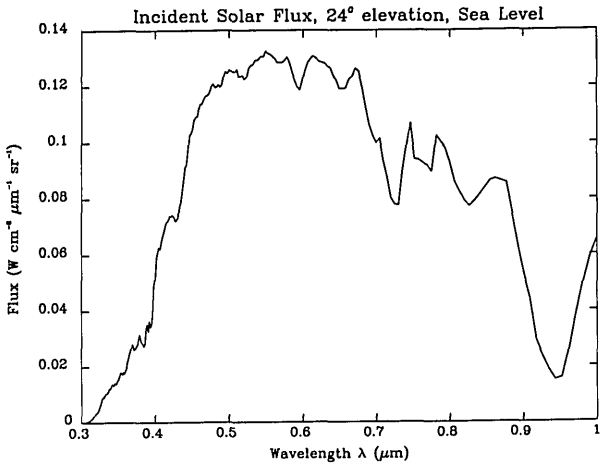

Fig. 1. Spectrum of incident sunlight at sea level with a solar altitude of 20°.

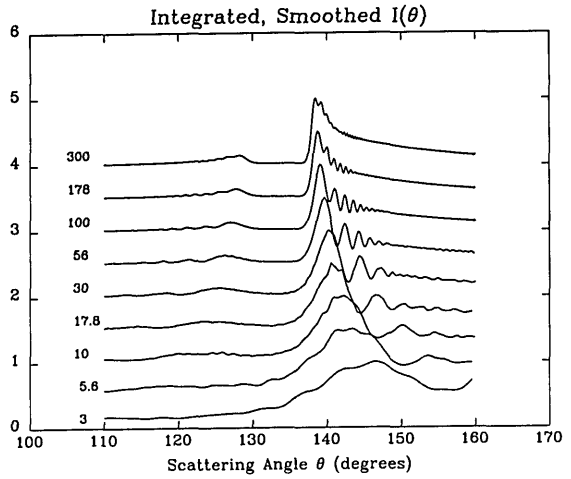

Fig. 2. $I(\Theta)$ with drop radius a as a parameter.

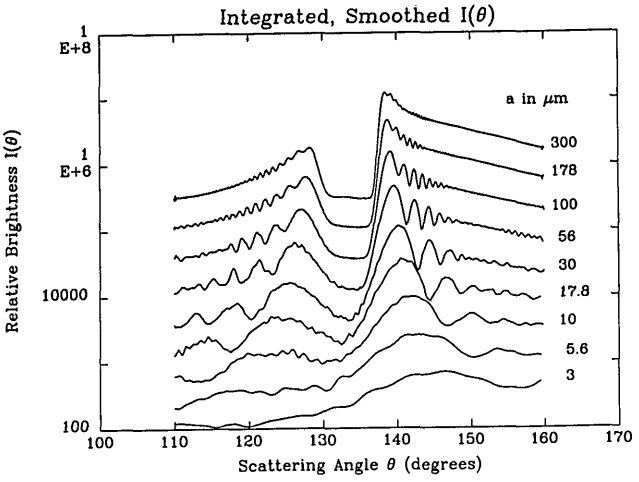

Fig. 3. Logarithm of $I(\Theta)$ with drop radius a as a parameter s11fda.plt (PAM).

approximately a factor of 5 compared with the Nyquist interval to avoid aliasing the results.

For each wavelength between and including 0.35–0.70 μm at 0.1-μm intervals, S_{11} was calculated and then multiplied by the incident solar flux $I_{\odot}(\lambda)$ at the wavelength calculated by LOWTRAN[11] for a solar elevation of 20° and a sea level observer (Fig. 1). Note that $I_{\odot}(\lambda)$ departs significantly from a smooth blackbody curve. The wavelength range was chosen to match approximately that of the eye and film, yet with the full understanding that we were not trying to predict what either of these media would actually record. Concern about aliasing by sampling such an irregular and sometimes steeply sloped spectrum at discrete intervals led us to try several smoothed versions of Fig. 1. Virtually no differences were found and the unsmoothed spectrum was used. After each matrix element was multiplied by the solar flux, all 36 products were added together to give the penultimate scattering function. Finally this integrated scattering function was smoothed (convolved) by a 0.5° boxcar window to simulate the effects of the finite angular width of the sun. Experiments with the true solar profile $S_{\odot}(\theta)$ showed negligible differences between the results obtained with it and with those from a 0.5° boxcar.

The diffraction limit of the drop $1.22\lambda/2a$ (and the characteristic size of the diffraction ripples) is equal to 0.5° for $a = 35\ \mu$m. Any structure whose angular size is much smaller than the sun's 0.5° diameter (smoothing function width) will be severely damped in amplitude while those that are much larger than 0.5° will be substantially unaltered.

III. General Results

Figure 2 shows $I(\theta)$ for particle radii 300, 178, 100, 56, 30, 17.8, 10, 5.6, and 3 μm corresponding to size parameters $x = 2\pi a/\lambda = 3770$, 2237, 1257, 704, 377, 224, 126, 70, and 380, respectively, for $\lambda = 0.5\ \mu$m. Figure 3 shows the logarithm of $I(\theta)$. The scattering functions are separated for clarity and are not representative of the true relative brightness $n(a)\pi a^2 Q_{sca} I(\theta)$, where $n(a)$ is the drop size distribution of interest. $I(\theta)$ is proportional to the bows' photometric radiance, e.g., W cm^{-2} sr^{-1}, in the 0.35–0.70-μm band.

Figures 2 and 3 show the primary rainbow near 138°, secondary bow near 129°, Alexander's dark band between the two, and supernumerary bows accompanying both the primary and secondary bows. As the drop radius a decreases a number of changes occur in both primary and secondary bows: their widths increase, their constrasts decrease, and their scattering angles of maximum brightness move away from Alexander's dark band. Alexander's dark band changes from having a flat bottom to having a U-shaped bottom.

The supernumerary bows grow wider and further apart with decreasing drop size. They also seem to show the highest contrast around a = 30–56 μm because at larger drop sizes the separation of the bows is much less than the sun's 0.5° diameter and their amplitudes are severely diminished. For smaller drop sizes, the supernumerary bows widen and lose contrast making their visibility decrease. The visibility of supernumerary bows in rain showers is critically dependent on drop size, shape, and distribution[12] as well as the coherence of the light reaching the drop.[13]

IV. Primary Rainbow, Secondary Rainbow, and Alexander's Dark Band

The position of the peak brightness of each rainbow as well as the positions of the half-power points relative to Alexander's dark band were measured and tabulated (Fig. 4, Table I) along with the width (= outer edge–inner edge) of the bows as well as several other parameters that we discuss shortly. The words inner and outer refer to the scattering angle, inner referring to smaller scattering angles. The dotted line in Fig. 7 shows the peak position of a monochromatic 0.6-μm rainbow based on the equation given in van de Hulst's Fig. 47,[4] $\theta = 138 + 20.9\, a_\mu^{-2/3}$. The peak brightness of the real bow would appear to fall at slightly smaller scattering angles than would the monochromatic bow.

If we define the edges of Alexander's dark band as the position of the inner primary bow and the outer secondary bow, Fig. 4 shows that the width of the band is nearly constant at ~9.5° regardless of drop size. This finding confirms earler suggestions[1] based on observations. For the band's width to remain constant, both the primary and secondary bows must grow away from Alexander's dark band with decreasing drop size.

Figure 5 shows the width (FWHM) of the primary and secondary bows as a function of drop size a. There is a minimum in the width of the rainbow for drop sizes around 100 μm, a result not previously known to the authors. The reason for the minimum may involve the presence of the supernumeraries[14] and their interaction with light from the outer part of the classical primary bow and with the finite width of the sun. For large drop sizes where the supernumerary bows are closely spaced, the smoothing caused by the sun's diameter causes the supernumerary light to be mixed with that from the classical primary and thus broadens the bow over what would be measured if the supernu-

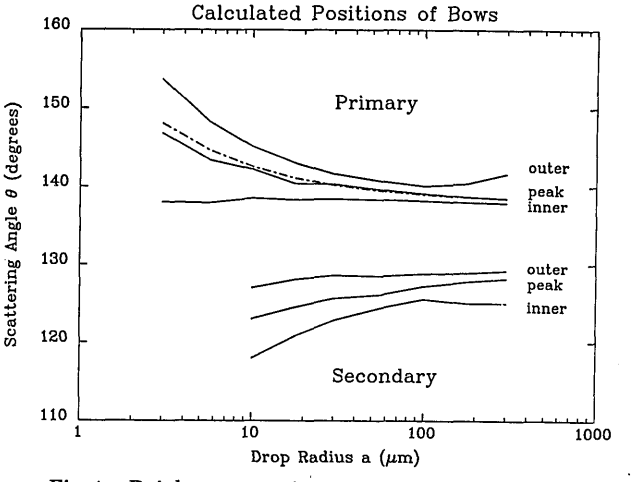

Fig. 4. Rainbow properties as a function of drop size.

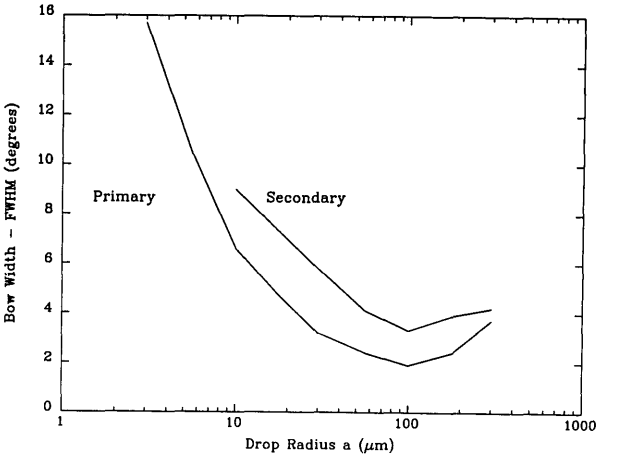

Fig. 5. Width of primary and secondary rainbows versus drop radius a.

Table I. Summary of Rainbow Calculations for the Primary and Secondary Bows[a]

a (μm)	Log a	x	Inner Edge (deg)	Peak Brightness (deg)	Outer Edge (deg)	Width (deg)	p_{max}
PRIMARY RAINBOW							
3	0.50	38	138.0	146.8	153.7	15.7	0.80
5.6	0.75	70	137.9	143.4	148.3	10.4	0.83
10	1.00	126	138.5	142.2	145.1	6.6	0.85
17.8	1.25	224	138.3	140.4	143.0	4.7	0.89
30	1.50	377	138.4	140.3	141.6	3.2	0.88
56	1.75	704	138.3	139.6	140.7	2.4	0.89
100	2.00	1257	138.2	139.1	140.1	1.9	0.87
178	2.25	2237	138.0	138.7	140.4	2.4	0.80
300	2.50	3770	137.9	138.5	141.6	3.7	0.78
SECONDARY RAINBOW							
3	0.50	38	—	—	—	—	—
5.6	0.75	70	—	—	—	—	—
10	1.00	126	(118)	(123.0)	(127)	(9.0)	0.45
17.8	1.25	224	120.8	124.5	128.1	7.3	0.47
30	1.50	377	122.8	125.6	128.6	5.8	0.47
56	1.75	704	124.4	126.1	128.5	4.1	0.50
100	2.00	1257	125.5	127.2	128.8	3.3	0.52
178	2.25	2237	125.0	127.8	128.9	3.9	0.53
300	2.50	3770	125.0	128.2	129.2	4.2	0.52

[a] —, Too indistinct for evaluation; ( ) an estimate, not a measurement.

meraries were absent. When the supernumerary spacing approaches the sun's angular diameter near $a = 35\ \mu m$, the supernumeraries do not blend with the primary and consequently the primary bow is narrower. For drop sizes smaller than $\sim 100\ \mu m$, the primary bow widens because a large portion of its energy may be viewed as coming from the zeroth-order supernumerary, i.e., the supernumerary that always sits atop the geometric bow. As the drop size decreases, the width of the supernumeraries increases and so does the primary bow. The prediction of a variable width of the natural rainbow certainly agrees with the authors' subjective impression, but we are unaware of any actual measurements that correlate rainbow width with drop size.[15]

V. Contrast and Color

The contrast $c = (I_p - I_A)/I_A$ of the bows, where I_p is the peak brightness and I_A is the mean brightness of Alexander's dark band, was measured as a function of drop radius and the results are shown in Fig. 6 and tabulated in Table I. From $a = 3\ \mu m$ to $a = 10\ \mu m$, the primary bow shows a nearly constant contrast but the secondary bow shows a low and probably undetectable contrast for a less than $\sim 10\ \mu m$. Because the primary bow widens rapidly with decreasing drop size, its apparently constant contrast does not mean that it is always visible. To be detected it must be seen against a uniform featureless background: high contrast, structured backgrounds will hide its subtle nature. For $a = 10\ \mu m$ to $a = 50\ \mu m$, the contrast undergoes a steep increase at around $a = 30\ \mu m$ for both bows and then levels off beyond about $a = 100\ \mu m$. With the contrast relatively high and the width at its minimum, the most easily discernible rainbow is expected to be those formed in drops with $a \sim 100\ \mu m$.

Figure 7 shows how blue ($\lambda = 0.4\ \mu m$) and red ($\lambda = 0.65\ \mu m$) monochromatic bows fall relative to one another for $a = 100\ \mu m$. Clearly the red bow is well separated from the blue bow. As the drop size grows narrower, the red and blue bows broaden and overlap, causing the bow to lose its color and grow whitish. We can define a color purity parameter $\phi = S/W$, where S is the angular separation of the peaks of the red and blue bows, and W is their average angular width (full width at half-maximum, FWHM). If $\phi = 0$ the colors totally overlap and the bow is white while values of ϕ exceeding 1 represent colorful bows. The precise values of ϕ do not depend strongly on the wavelengths chosen for red and blue providing that they are near opposite ends of the visible spectrum. Figure 8 shows how the color purity parameter ϕ varies with drop radius a. For drops larger than $\sim 100\ \mu m$, the bow shows good colors and the most colorful bows should be those with the largest drops. For $a = 50\ \mu m$ or less, $\phi < 0.5$ and bows are pale and faded.

VI. Supernumerary Bows

The scattering angle of peak brightness was measured for the primary and secondary supernumerary bows. The job was more difficult than for the primary and

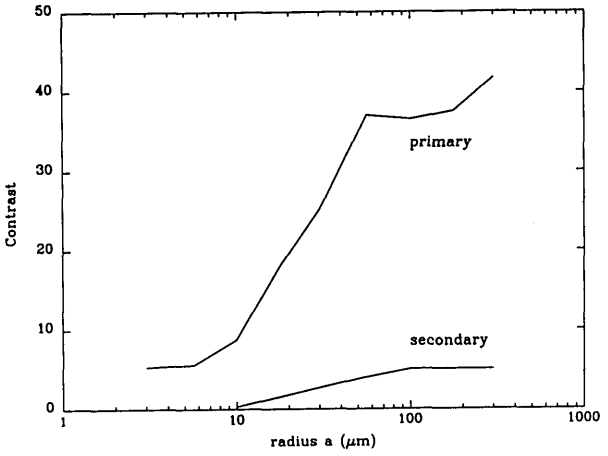

Fig. 6. Contrast versus drop radius a.

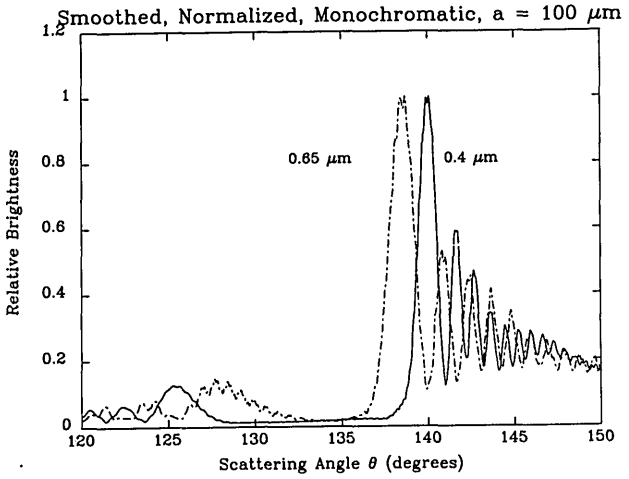

Fig. 7. Monochromatic bows at a wavelengths of 0.40 and 0.65 μm for $a = 100\ \mu m$.

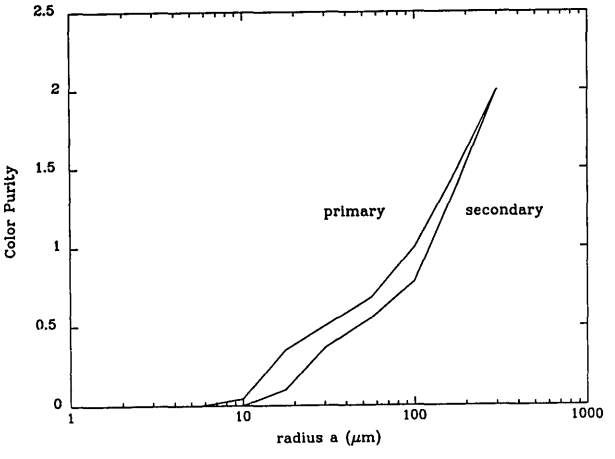

Fig. 8. Color purity parameter ϕ vs drop radius a.

secondary bows because fine structure in the bows sometimes made it difficult to unambiguously identify the desired parts of $I(\theta)$. The results are also presented in Table II and shown graphically in Fig. 9. As expected from experience, the location of the supernumerary bows changes monotonically with drop size.

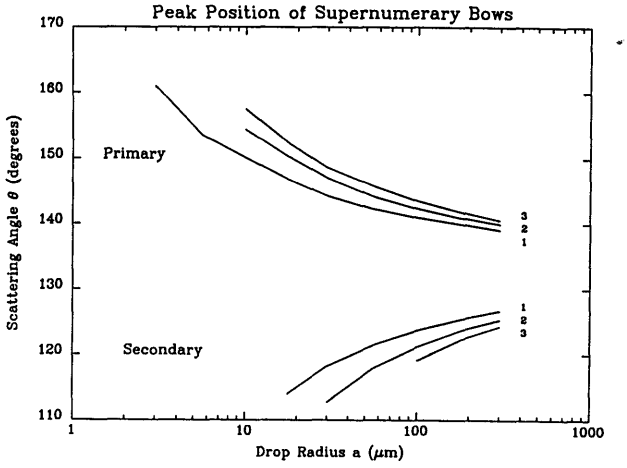

Fig. 9. Position of supernumeraries.

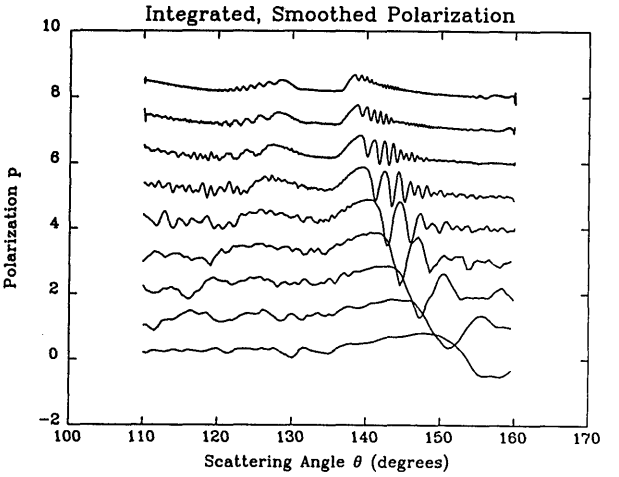

Fig. 10. Polarization p vs drop size.

VII. Polarization

The degree of linear polarization p is shown in Fig. 10. The polarization curves in Fig. 10 resemble those of $I(\theta)$ in Figs. 2 and 3 because, in general, brightness and polarization correlate for transparent drops in this range of scattering angles. Figure 11 shows the maximum polarization (which occurs at the peak brightness of the bows) as a function of drop size. The maximum polarization reaches a maximum of 90% for the primary bow and 50% for the secondary for drop radii between 20 and 100 μm. Significant polarization exists in the bows, especially the secondary bows, even when the contrast has dropped below the level of visibility. Thus a uniform, featureless cloud deck illuminated by the sun might not show any rainbow but would be expected to display significant polarization near the rainbow angle.

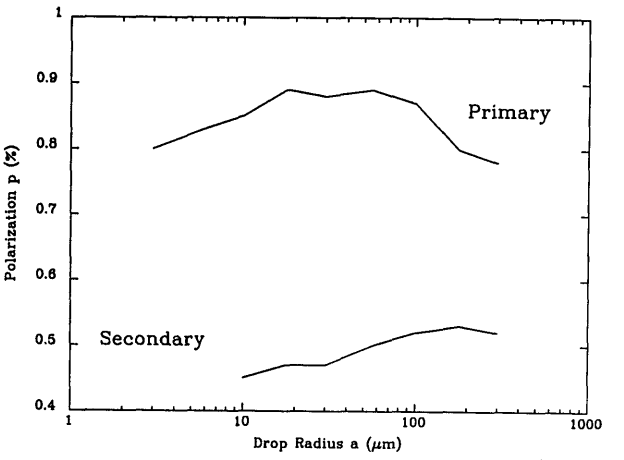

Fig. 11. Maximum linear polarization.

VIII. Definition of a Fogbow

How does one define a fogbow? In most peoples' minds, a fogbow is a nearly white or almost colorless rainbow and it is perhaps here (Fig. 8) that we should take our starting point. The red and blue rainbows begin to overlap one another significantly when the drop radius is less than ~100 μm and we already know that there is a width minimum in the rainbow (Fig. 5) at a = 100 μm. At a = 35 μm, the FWHM of the diffraction ripple size equals the width of the sun, i.e., 0.5°. A survey of the fogbow literature shows that the mean drop radius reported is always <60 μm, and usually ranges from 25 to 50 μm. Thus we might tentatively suggest that a fogbow is any rainbow formed in drops whose radii are 35 μm or less. Such a definition is compatible with our experience, consistent with the theoretical calculations presented above,

Table II. Summary of Rainbow Calculations for the Supernumerary Bows[a]

	Peak Positions of Supernumerary Bows						
	Primary				Secondary		
a	1	2	3	4	1	2	3
3	161	—	—	—	—	—	—
5.6	153.5	—	—	—	—	—	—
10	150.1	154.4	157.5	—	—	—	—
17.8	146.8	150.3	152.4	154.8	(114)	—	—
30	144.3	147.0	148.6	—	118.2	112.7	—
56	142.3	144.2	145.8	—	121.5	118.0	—
100	141.0	142.4	143.6	144.5	123.7	121.2	119.1
178	140.0	141.0	141.9	—	125.4	123.7	122.3
300	139.1	140.0	140.6	—	126.7	125.3	124.3

[a] —, Too indistinct for evaluation; ( ), an estimate, not a measurement.

and yet has a precise and physically meaningful basis: the diffraction limit of a circular aperture whose FWHM matches the solar diameter.

IX. Summary and Conclusions

We have calculated the scattering matrix element S_{11}, polarization p, and the expected integrated angular scattering function $I(\theta)$ for scattering angles of 110–160° for monodisperse water drops. The range of sizes used was between 3 and 300 μm ($3800 > X > 38$). We improved on previous calculations by the addition of two aspects of solar illumination: the solar spectrum as modified by the earth's atmosphere and the finite angular size of the sun. To use the results presented here to model a rainbow formed in a shower with a range of drop sizes, it is necessary to weight the $I(\theta)$ functions with $n(a)Q_{sc}\pi a^2$.

We did not include the effects of multiple scattering or a range of drop sizes because neither effect can be specified with any degree of uniqueness: light may be scattered any number of times and the distribution of drop sizes varies over enormous ranges. Nor did we attempt to modify the calculations to try to mimic the response of either the eye or film, although these factors are necessary to make quantitative comparison between theory and observation (visual or photographic). We believe, however, that our results will be a faithful guide to visual or photographic observers. Our main findings are the following:

(1) The rainbow reaches a minimum width for $a = 100$ μm.

(2) The supernumerary bows of the primary reach maximum visibility for $a = 50$ μm.

(3) Alexander's dark band remains at a constant width of 9.5° although its shape changes with drop size.

(4) The maximum linear polarization of both bows varies with drop size.

(5) The secondary fogbow can only be seen when $a > 10$ μm.

We suggest that a fogbow be defined as any rainbow formed in drops less than $a = 35$ μm.

We thank Steve Mazuk for his able software assistance in calculating the 40 million Bessel functions that formed the basis of this work. We are grateful to two reviewers for their many useful comments.

References

1. The best set of quantitative observations of natural fogbows seems to be that from Ben Nevis published in 1887 by Omond in the Proceedings of the Royal Society of Edinburgh and analyzed by J. C. McConnell, "The theory of fog-bows," Philos. Mag. **29**, 453–461 (1890).
2. G. H. Liljequist, "Halo phenomena and ice crystals," Norwegian-British-Swedish Antarctic Expedition, 1949–1952, Scientific Results, Vol. 2, Part 2, Special Studies (1956); F. Palmer, "Unusual rainbows," Am. J. Phys. **13**, 203–204 (1945); R. A. Brown "Occurrence of supernumerary fogbows at subfreezing temperatures," Mon. Weather Rev. **94**, 47–48 (1966); W. C. Livingston, "The cloud contrast bow as seen from high flying aircraft," Weather **34**, 16 (1979).
3. A. de Ulloa, "Relazion historica del viage á la America meridional," Part 1, Section 2, 592–593 (1748).
4. H. C. van de Hulst, *Light Scattering by Small Particles* (Wiley, New York, 1957; reprinted by Dover, New York, 1981).
5. C. W. Querfeld, "Mie atmospheric optics," J. Opt. Soc. Am. **55**, 105–106 (1965).
6. J. E. Hansen and L. D. Travis, "Light scattering in planetary atmospheres," Space Sci. Rev. **16**, 527–610 (1974).
7. C. F. Bohren and D. R. Huffman, *Absorption and Scattering of Light by Small Particles* (Wiley-Interscience, New York, 1983).
8. W. M. Irvine and J. B. Pollack, "Infrared optical properties of water and ice spheres," Icarus **8**, 324–360 (1968).
9. J. E. MacDonald, "The shape and aerodynamics of large raindrops," J. Meteorol. **11**, 478–494 (1954); A. W. Green, "An approximation for the shape of large raindrops," J. Appl. Meteorol. **14**, 1578–1583 (1975).
10. K. V. Beard, H. T. Ochs, and R. J. Kubesh, "Natural oscillations of small raindrops," Nature (London) **342**, 408–410 (1989).
11. F. X. Kneizys, E. P. Shettle, L. W. Abreu, G. P. Anderson, J. H. Chetwynd, W. O. Gallery, J. E. A. Selby, and S. A. Clough, "Users guide to LOWTRAN7," AFGL-TR-88-0177 (U.S. Air Force Geophysics Laboratory, Bedford, Mass., 1988).
12. F. E. Volz, "Some aspects of the optics of rainbows and the physics of rain," in *Physics of Precipitation* (American Geophysica Union, Washington, D.C., (1960), pp. 280–286 A. B. Fraser, "Inhomogeneities in the color and intensity of the rainbow," J. Atmos. Sci. **29**, 211–222 (1972); "Why can the supernumerary bows be seen in a rain shower?" J. Opt. Soc. Am. **73**, 1626–1628 (1983).
13. J. A. Lock, "Observability of atmospheric glories and supernumerary rainbows," J. Opt. Soc. Am. A **6**, 1924–1930 (1989).
14. In the geometric limit, the angle of minimum deviation represents a hard limit like an opaque edge. We know from wave theory that such an edge results in diffraction that puts light into the shadow, or in this case into smaller deviation angles. The spacing of the diffraction ripples is small for large drops. For large drops there will be many diffraction ripples sitting on top of the geometric rainbow. Because they are faint, they are not generally noticed. However, with decreasing drop size, the diffraction ripples increase in visibility (width and contrast) until a point is reached where the first-order diffraction ripple (=zeroth supernumerary) matches the contribution from the classical rainbow. For smaller drops yet diffraction dominates and the rainbow, by now faint and pale, results almost exclusively from diffraction.
15. There seems to be little in the way of reliable measurements of the natural rainbow's width in the literature. Most discussions refer to the width being ~2°, apparently based on the difference between the angles of minimum deviation for red and blue light [e.g., R. A. R. Tricker, *Meteorological Optics* (American Elsevier, New York, 1970), who suggests a width of 1.7.]. However, when the solar distribution of energy and finite width to the sun's diameter are included, the bow widens considerably.